



HAL
open science

Trace elements and graphite shape degeneracy in nodular graphite cast irons

Jacques Lacaze

► **To cite this version:**

Jacques Lacaze. Trace elements and graphite shape degeneracy in nodular graphite cast irons. International Journal of Metalcasting, 2017, vol. 11 (n° 1), pp. 44-51. 10.1007/s40962-016-0115-6 . hal-01580435

HAL Id: hal-01580435

<https://hal.science/hal-01580435v1>

Submitted on 1 Sep 2017

HAL is a multi-disciplinary open access archive for the deposit and dissemination of scientific research documents, whether they are published or not. The documents may come from teaching and research institutions in France or abroad, or from public or private research centers.

L'archive ouverte pluridisciplinaire **HAL**, est destinée au dépôt et à la diffusion de documents scientifiques de niveau recherche, publiés ou non, émanant des établissements d'enseignement et de recherche français ou étrangers, des laboratoires publics ou privés.



Open Archive TOULOUSE Archive Ouverte (OATAO)

OATAO is an open access repository that collects the work of Toulouse researchers and makes it freely available over the web where possible.

This is an author-deposited version published in: <http://oatao.univ-toulouse.fr/>
Eprints ID : 18120

To link to this article: DOI: 10.1007/s40962-016-0115-6
URL: <http://dx.doi.org/10.1007/s40962-016-0115-6>

<p>To cite this version: Lacaze, Jacques <i>Trace elements and graphite shape degeneracy in nodular graphite cast irons.</i> (2017) International Journal of Metalcasting, vol. 11 (n° 1). pp. 44-51. ISSN 1939-5981</p>

Any correspondence concerning this service should be sent to the repository administrator: staff-oatao@listes-diff.inp-toulouse.fr

TRACE ELEMENTS AND GRAPHITE SHAPE DEGENERACY IN NODULAR GRAPHITE CAST IRONS

Jacques Lacaze 

CIRIMAT, ENSIACET, Université de Toulouse, Toulouse, France

DOI 10.1007/s40962-016-0115-6

Abstract

Graphite degeneracy in spheroidal graphite cast iron is a common issue faced by foundries. It is generally associated with the presence of so-called poisoning elements and may in some cases be suppressed by the addition of other elements. Mastering these additions is not simple in practice since industrial alloys do generally contain many elements that can affect graphite shape even when present at low or trace levels. In this work, trace and

low-level elements are considered in relation with three steps of microstructure formation: (1) nucleation of graphite; (2) growth of graphite; and (3) solid-state transformations.

Keywords: nodular graphite cast iron, graphite degeneracy, trace elements, eutectoid reaction

Introduction

The role of low-level elements on solidification of cast irons has been the subject of many reviews^{1–4} and remains a major topic in cast iron research and development. One obvious problem is quantifying low-level elements as they may be effective below the detection limits of standard or even advanced analytical means. Further, chemical analyzes, e.g., induction coupled plasma analysis or X-ray fluorescence, are global and do not give any hint on where and how trace elements have affected microstructure formation. Emphasis has thus often been put on characterizing related compounds and to make some assumptions on the mechanism of their action. This contribution will first discuss aspects related to trace element effects when dealing with nuclei formation. The discussion will then be extended to graphite growth during solidification, and finally some comments will be made on solid-state transformation. It is not intended to provide an exhaustive review of the literature, but instead to support selected evidences and to stress pending questions.

Graphite Nucleation

The possible inoculation mechanisms in spheroidal graphite cast irons have been thoroughly reviewed by Skaland⁵ following previous work which proposed a three-

step model where a core of sulfide gets surrounded by an oxide shell on top of which a complex $XO \cdot MgO \cdot SiO$ oxide precipitates (Figure 1a), where X may be Al, Ca or Ba.⁶ The understanding of the role of oxi-sulfides in the building up of appropriate nuclei led to the definition of new inoculants doped with S and O and containing elements reacting with them such as Ca and rare earths (RE).⁷ In the same line, Suarez et al.⁸ have made late addition of 0.012 mass% S to a high-silicon spheroidal graphite iron (SGI) and observed an increase in the nodule count with respect to the melt without such an addition.

A somehow simpler mechanism involving a core made of MgO encapsulated in MgS has been proposed by Igarashi and Okada⁹ who analyzed nuclei in SGI with advanced analytical techniques. They found that the nuclei exist in a small MgO core surrounded by a (Mg,Ca)S rounded particle about 1 μm in diameter (Figure 1b), with additionally some small (Mg,Si,Al)N nitrides attached. The authors stressed that their observations are in agreement with previous works—among which that by Lalich and Hitchings¹⁰—in that graphite appears to nucleate on sulfides. On the contrary, they are at change with the conclusion by Skaland et al.⁶ and this discrepancy has later been ascribed by Nakae and Igarashi¹¹ to the very low sulfur content of the cast iron used by Skaland et al. (0.002–0.004 mass% S).

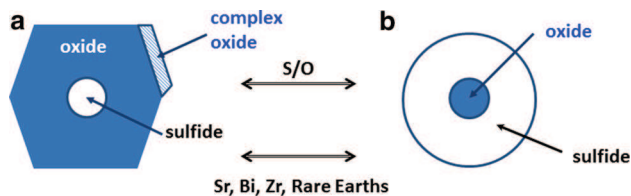


Figure 1. Schematic of nuclei formation according to Skaland⁶ (a) and to Igarashi and Okada⁹ (b). The upper double arrow stresses that the switch from one model to the other may depend on the O and S content of the melt. The lower double arrow suggests that other minor elements introduced in inoculants may further shift the limit between the two models.

From their observations, Igarashi and Okada⁹ stressed three points:

1. MgO and (Mg,Si,Al)N do not seem to help graphite nucleation. It has been established that this latter phase could eventually turn to become nuclei in low-S melts¹¹ and that it has an approximate composition given by $\text{AlMg}_{2.5}\text{Si}_{2.5}\text{N}_6$ with a trigonal structure very close to the hexagonal AlN structure.¹² This composition differs from $\text{Al}_4\text{Mg}_{30}\text{Si}_{32}\text{N}_{34}$ measured by Mercier et al.¹³ who suggested the formula MgSiN_2 which is in fact not far from the formula proposed by Nakae and Igarashi.
2. RE were not detected which is somehow astonishing as Nakae and Igarashi¹¹ observed RE sulfides when using very similar nodularizing and inoculating alloys. This may be due to the very low amount of such RE-bearing sulfides which appear as small particles at the surface of the (Mg,Ca)S sulfides.
3. The MgS sulfides may have been liquid when graphite nucleated as indicated by their often rounded shape. This is the same conclusion as Horie et al. arrived at.¹⁴ Note that such rounded sulfide nuclei can be seen in the work by Lalich and Hitchings,¹⁰ Francis¹⁵ and Kusakawa.¹⁶ Further, Igarashi and Okada⁹ suggested that the separation of (Mg,Ca)S sulfide and RE-bearing sulfides occurs after the formation of graphite. Such a demixing happens because of miscibility gaps in S-rich or/and O-rich metallic liquids.

At very high sulfur content (0.083 mass%), Nakae and Igarashi observed faceted (Mg,Mn)S sulfides acting as nuclei for graphite. It thus appears that the state of the sulfide, either liquid or solid, at the time of formation of graphite does depend on its composition. Figure 2 shows the nucleus of a graphite spheroid found in an industrial nodular cast iron.¹⁷ This nucleus consists mainly of (Ca,Mg)S, but is amorphous and was certainly liquid when graphite nucleated. As mentioned above, several small particles of crystalline phases can be seen at the periphery

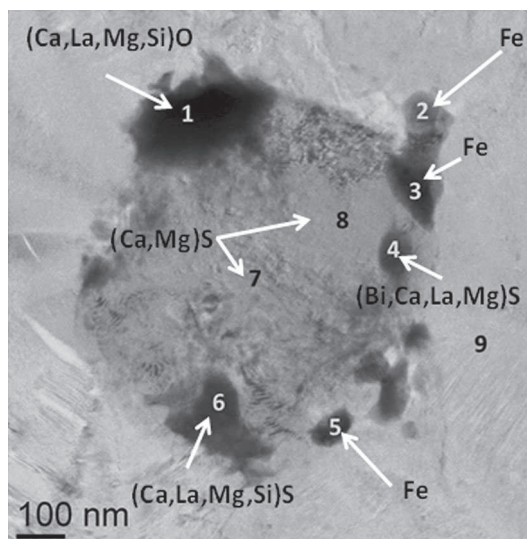


Figure 2. Graphite nucleus with an amorphous sulfide core (adapted from Theuwissen et al.¹⁷).

of this nucleus. They are enriched in strong deoxidizers and desulfurizers which have high atomic mass. It can thus be argued such additions counter flotation and fading of nuclei.

A last note concerning Figure 2 is that graphite developed as sectors right at the surface of the nucleus, but no epitaxy could be found between any of the dark crystalline precipitates and the graphite around.¹⁷ This suggests that graphite could certainly nucleate on any heterogeneous substrate and that the most important step in the nodularizing process is graphite growth as already pointed out by various authors.^{10,11} This will be further elaborated in the next section.

Many of the trace elements give rise to precipitation of oxides, sulfides, nitrides, carbides or other compounds, so that the amount of these elements remaining dissolved in the cast iron melt may greatly differ from analytical results. As a matter of fact, the amount of an element dissolved in the melt relates to the solubility limits for precipitation of the compounds which depend on thermodynamics, and to reaction kinetics which have not been thoroughly investigated. As an example, attempts to evaluate experimentally the amount of free Mg—i.e., dissolved in the liquid—have been performed by Hecht and Nonon¹⁸ for control of compacted graphite and Suárez et al.¹⁹ for control of nodular graphite.

In their study on inoculation of nodular cast iron, Skaland et al.⁶ evaluated the number of particles assuming all S goes in MgS and all O in complex silicates. They noted that this number is about 10 times higher than the nodule count. For a volume fraction of graphite at about 10 %, this agrees with Mercier et al.¹³ who have counted inclusions present in the matrix and in graphite and found the same number of

inclusions for a given surface of either phase. At increasing RE addition, Onsoien et al.²⁰ noticed that the complex oxysulfide (Figure 1a) get replaced by Mg–Si bearing particles that become nuclei at much larger undercoolings than the former ones. Though the melt composition was changed in their study, their result raises the question of secondary nucleation in cast irons. Modern analytical means should allow investigating if the composition of graphite nuclei remains the same during solidification of a given cast iron. Such knowledge should help improving the available models for graphite nucleation with some hope that graphite nodule size distribution could be properly simulated.

Graphite Growth

Whatever the nuclei are, graphite shape depends solely on its growth step. In this instance, it is agreed that the first effect of the nodularizing treatment is to fix most of the O and S dissolved in the melt. The other way around, this has led to consider these latter elements as those favoring lamellar growth. However, there is a wealth of evidence that these two elements adsorb differently at the surface of graphite, and this may be an indication that their action on graphite growth is not the same. Direct experimental evidence by Franklin and Stark²¹ using secondary ion mass spectroscopy (SIMS) has a high analytical resolution for most elements (see Figure 3) though it is not quantitative. From their results on lamellar graphite, it could be concluded that oxygen prefers to adsorb on the prismatic planes and is thus homogeneously distributed in bulk graphite, while sulfur adsorbs on basal planes and appears accumulated at the interface between the graphite layers constituting the lamellas. Results by Park and Verhoeven²² using Auger analysis confirmed this conclusion for sulfur, while the authors thought that the thick oxygen build up they observed along the prismatic planes may have occurred after solidification.

The graphite layers mentioned above may be seen as so-called structural base units (SBU) which develop along the prismatic direction of graphite as schematically illustrated in Figure 4. In well-formed primary graphite lamellas, these SBUs can be up to several tens of micrometers long, while their thickness is in the range of a few hundred nanometers to a couple of microns. Graphite lamellae are made up of SBUs stacked upon each other. After doping a Fe–C melt with Sb, it was found that graphite lamellas

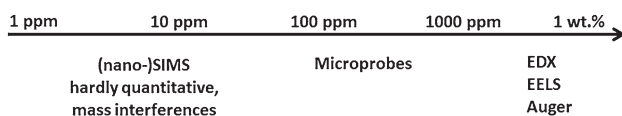


Figure 3. Detection limits of various micro-analytical techniques of secondary ion mass spectroscopy (SIMS), electron microprobes, energy dispersive spectroscopy (EDX), electron energy loss spectroscopy (EELS) and Auger.

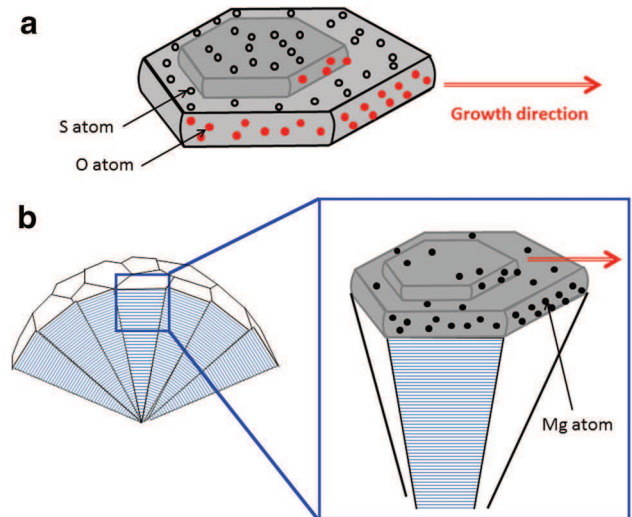


Figure 4. Schematic of lamellar (a) and spheroidal (b) graphite growth.

became wavy and transmission electron microscopy (TEM) observation showed this to be associated with a marked shortening of the SBUs without noticeable change of their thickness.^{23–25}

Other forms of graphite in cast irons may be seen to be similarly made of stacking of SBUs. This was long ago postulated for spheroidal graphite by Mitsche et al.²⁶ and demonstrated with transmission electron microscopy (TEM) by Miao et al.²⁷ The schematic of compacted graphite proposed by Den Xijun et al.²⁸ and the scanning electron microscopy (SEM) observations by Geier et al.²⁹ may be similarly understood. TEM observations of chunky graphite showed the same thing³⁰ which appears well in line with the schematic proposed by Loper et al.³¹ for this degenerate graphite. From the above observations, it may be concluded that graphite growth in cast irons always proceeds along the prismatic direction, whatever is the apparent growth direction that the overall shape suggests. In the case of spheroidal graphite, for example, the overall shape would suggest graphite grows along the basal plane direction (*c* axis), but the detailed observation of its internal structure leads to conclude the growth mechanism is along the prismatic direction. The further observation that screw dislocations cannot explain spheroidal growth^{32,33} suggested a mechanism involving continuous nucleation of new SBUs at the outer surface of the nodules and their lateral growth along the prismatic direction, see Figure 4b. An indirect support to this model was given by its ability to describe the formation of exploded graphite during flotation.³⁴

Nodularizing elements—i.e., magnesium and RE—not only fix O and S as stable compounds precipitating in the melt, but they also affect graphite growth. This is clearly demonstrated by the fact that over-treatment with either Mg or RE leads to graphite degeneracy. When studying

graphite flotation, Sun and Loper³⁵ noticed that exploded nodules in RE-treated melts were three times smaller than in Mg-treated melts at given casting conditions. This suggests that nodularizing elements hinder graphite growth as reported long ago by Sidorenko et al.³⁶ Note also that this may well explain that nodularizing elements promote carbide formation by limiting the kinetics of the stable eutectic solidification from Figure 4b, it is thus postulated that nodularizing elements adsorb at graphite/melt interface along the prismatic planes during SBU growth, being then partly absorbed in graphite.

With the aim of understanding graphite growth mechanism and the role of trace elements, attempts for analyzing the composition of graphite precipitates have been performed for a long time. One of the successful techniques is extracting graphite precipitates, burning them and analyzing the ashes by standard chemical analysis. This technique has been used long ago³⁷ and renewed by Francis¹⁵ who complemented it with SEM and TEM examinations and local analyzes with energy dispersive spectrometry (EDX). Francis made reasonable assumptions to separate the contributions of the nuclei and of graphite. His data demonstrates that many elements are present in bulk graphite, but a close examination does not show any clear difference between lamellar and nodular graphite.

Locating trace elements within graphite and at the graphite/matrix interface with SIMS analysis has been attempted by Fidos,^{38,39} Franklin and Stark²¹ and more

recently Lacaze et al.,⁴⁰ and with scanning proton analysis by Feng Songli et al.⁴¹ Fidos attempted to quantify his results by simulation and reported values for slow cooled (186 °C/min) and fast cooled (382 °C/min) cast irons. The changes in the results between these two cast irons appear, however, by far too large to be explained by the limited change in cooling rate and may thus be attributed to scattering in the measurements. The conclusions of the above studies seem to be that any element present in the melt is prone to enter to some level in graphite and that there is no significant accumulation at the graphite melt interface.

In order to clarify the role of various elements on graphite growth, doping of synthetic Ni-C alloys^{42,43} and Fe-C alloys^{23,42,44} has been used. Exotic or interesting graphite precipitates could thus be obtained, such as exploded nodules illustrated in Figure 5 which were observed in a Fe-C-Ce alloy.²⁵ In these precipitates, the sectors of the graphite nodule appear well formed but separated from one another. This goes in line with Ce adsorbing on the prismatic planes along the graphite/liquid interface and slowing down the growth along the prismatic direction.

One way of rationalizing the effect of trace elements would be following Minkoff and Lux⁴⁵ and Munitz and Nadiv⁴³ who classified impurities as having strong interaction, weak or no interaction with graphite. Elements having strong interaction adsorb tightly at the graphite surface and get later absorbed uniformly within graphite. Munitz and Nadiv⁴³ note this is the case of La and Ca which are on the

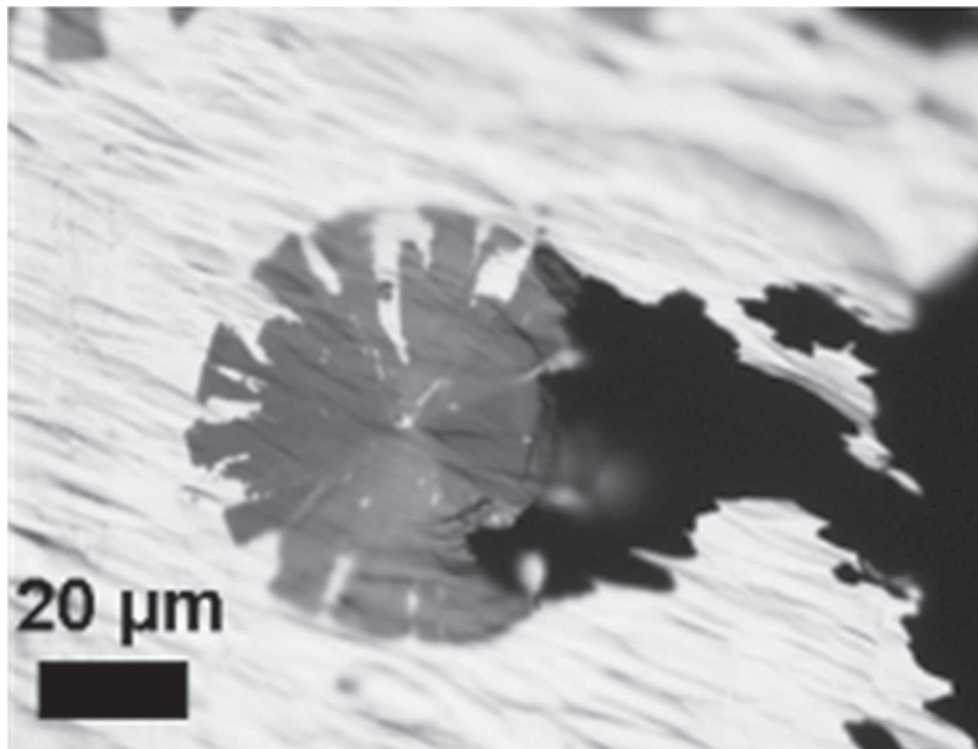


Figure 5. Thin foil of an exploded nodule extracted from a Fe-C-Ce alloy.²⁴

left of the periodic table. This should also be the case of Ce and Mg which are on the left of the table as well. Weak interaction elements are adsorbed on graphite surface by van der Waals' forces, and they are thus quite mobile and should accumulate at the graphite outer surface during its growth. According to Munitz and Nativ⁴³ this is the case of Pb, S, Bi, Se and Sb which are all on the right side of the periodic table. The authors could effectively point to a strongly different distribution of La and Pb in graphite grown from a Ni-C melt doped with 0.02 mass% La and 3.5 mass% Pb. While the result for La is clear, it may be that the surface accumulation of Pb relates to precipitation of pure Pb (demixion of the liquid) as indicated by the authors. Such a line of thinking could be supported by atomistic calculations if they could be made representative of graphite/iron melt interface.

Solid-State Transformations

The discussion below concerns only the formation of ferrite and pearlite which are the most common constituents of the matrix of cast iron parts. In the temperature range of the stable and metastable eutectoid reactions, long-range diffusion of substitutional solutes is so sluggish that it cannot take place during continuous cooling provided the cooling rate is larger than about 1–2 K/min.⁴⁶ Accordingly, ferrite or pearlite should inherit the content in substitutional solutes of the parent austenite⁴⁷ as recently experimentally investigated.⁴⁸ Growth of ferrite is thus controlled by carbon diffusion from the ferrite/austenite interface to the ferrite/graphite interface, even though some carbon may also be redistributed in austenite. Such a process can take place only when the temperature of the material is below the lower limit of the three-phase field (austenite + ferrite + graphite) denoted T_x . The pearlite promoter effect of Cu, Mn and Ni may be rationalized as due to the lowering of T_x , and thus of the rate of carbon diffusion. In the case of Mn, this temperature effect is enhanced by a marked decrease in the carbon difference—and thus the driving force for carbon diffusion—between the two interfaces.⁴⁹

It has also been proposed that growth of pearlite may proceed only when the temperature of the material is below the lower limit of the metastable three-phase field (austenite + ferrite + cementite) denoted T_p .⁴⁷ Interestingly enough, review of literature data showed that the growth rate of pearlite is the same for cast irons containing various levels of As, Cu, Mn and Sn.⁵⁰ This suggests that growth of pearlite is mainly controlled by redistribution of silicon between ferrite and cementite. Minor elements are known to affect the structure of the matrix, and this has been quantified long ago by Thielemann⁵¹ who expressed the amount of ferrite f^{fer} as an exponential function of the parameter Px which depends on composition:

$$f^{\text{fer}}(\%) = 961 \cdot \exp(-Px)$$

$$Px = 3.00 \cdot w_{\text{Mn}} - 2.65 \cdot (w_{\text{Si}} - 2.0) + 7.75 \cdot w_{\text{Cu}}$$

$$+ 90.0 \cdot w_{\text{Sn}} + 357 \cdot w_{\text{Pb}} + 333 \cdot w_{\text{Bi}} + 20.1 \cdot w_{\text{As}}$$

$$+ 9.60 \cdot w_{\text{Cr}} + 71.7 \cdot w_{\text{Sb}}$$

where w_i is the content (mass%) of element i .

It is seen in the expression of Px that Sn and Sb are effective at levels about ten times smaller than Cr, Cu and Mn, and Pb and Bi at levels which are about 50–100 times smaller. This suggests three classes of elements in relation to ferrite/pearlite formation:

- those as Si, Cr, Cu and Mn which have an alloying effect that can be described with the appropriate phase diagram;
- those as Sn and Sb which have been claimed to get accumulated at the graphite/matrix interface. Though such an enrichment may be controversial, it has been suggested that Fe-Sn or Fe-Sb compounds could form and this would be in line with the conclusion drawn from experiments that Sn higher than 0.05 mass% strongly decreases the undercooling necessary for pearlite nucleation.⁵²
- Finally elements such as Pb and Bi are effective at a very low level. It is here suggested that they adsorb at the graphite surface and block sites for carbon deposition, thus hindering ferrite growth and favoring the metastable transformation.

There is an issue about elements adsorbing at the graphite surface and accumulating at the graphite/matrix interface. As calculated by Double and Hellowell,⁵³ very low levels of trace elements would suffice to cover all graphite precipitates with a one atom-thick layer. If such elements had adsorbed during the solidification step, they would have totally hindered carbon transfer and thus led to metastable solidification. As this is not the case for common cast iron compositions, one should consider that (part of) both adsorption and accumulation proceed in solid state. This may be very much alike grain boundary segregation and would be worth specific research. In fact, such segregation of Mg has been evidenced by Dierickx et al.⁵⁴ as a result of solid-state heat treatment of SGI.

There are several other elements which do not appear in Px that are known to affect the constitution of the matrix. Some of them could be added using Mn-equivalent or Sn-equivalent published in the literature.⁵⁵ Sulfur also is such an element known to increase the amount of pearlite in malleable irons,⁵⁶ lamellar irons,⁵⁷ compacted and nodular irons.⁵⁸ Nakae⁵⁹ and Ying Zou⁶⁰ demonstrated that a S-free lamellar cast iron is fully ferritic when a common lamellar iron would be nearly fully pearlitic for the same casting conditions. Assuming S adsorbs preferentially on basal planes in solid state as concluded for solidification, this would mean it hinders the formation of new graphite steps

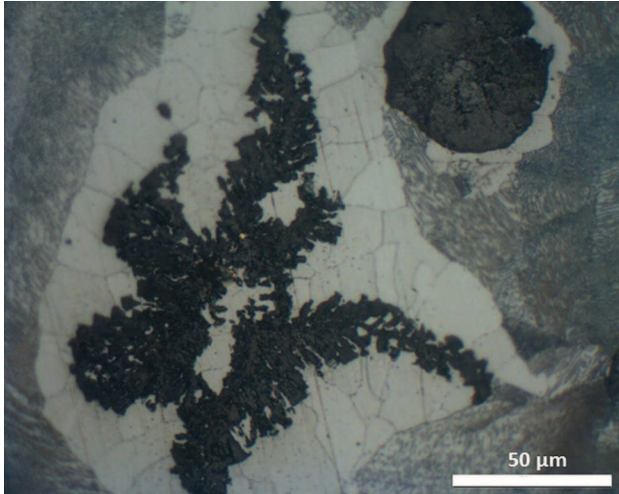


Figure 6. Microstructure observed in the riser of a standard ductile cast iron part (courtesy of AZTERLAN). The sample was Nital-etched, ferrite is white, while pearlite appears gray.

on top of the existing basal planes, thus hindering the development of new prismatic faces where carbon atoms could reach graphite precipitates. It is worth mentioning that this effect of sulfur is in fact used industrially to avoid metal dusting of pipes submitted to high carbon activity.^{61,62} This goes also with the strong adsorption of sulfur on graphite basal planes shown by scanning tunneling microscopy⁶³ and by atomistic calculations.⁶⁴ It may be of interest to mention that P, Sn and Cu have also been reported to be protective against metal dusting.⁶⁵

The role of the surface of graphite precipitates on the eutectoid transformation, and more particularly the fact that prismatic planes are facing the matrix, is illustrated with the micrograph in Figure 6. This micrograph was made on a section of the riser of a standard nodular cast iron part. It shows a large complex-shaped (degenerate) graphite precipitate nearing a well-formed nodule. Etching of the sample shows a significant growth of ferrite around the degenerate graphite, while only a thin halo of ferrite has formed around the nodule, and this difference may be definitely associated to the very many areas of the degenerate graphite precipitate having prism planes facing the matrix. Such a situation would arise when austenitizing a lamellar graphite iron because partial dissolution of graphite leads to new prism planes facing the matrix.⁶⁶ Also, and for that precise reason, one may understand why it is known to be so difficult to get a fully pearlitic matrix with as-cast compacted graphite irons. The above features have also been discussed by Gorny.⁶⁷

Conclusion

Based on selected information from literature, this paper has raised a number of questions which could be solved in

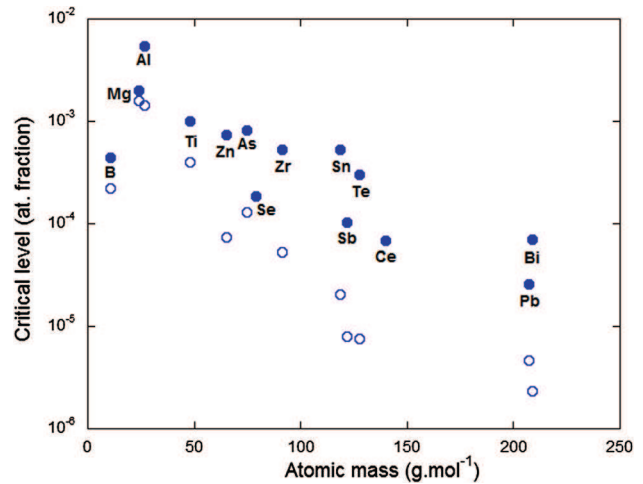


Figure 7. Relation between atomic mass of elements poisoning nodular irons and their reported critical levels.⁵⁵ Open symbols relate to minimum values seen to affect graphite shape, solid symbols to maximum admissible values.

the future either theoretically or by laboratory experiments and analyses. Plotting the critical level of various elements for graphite degeneracy in nodular irons⁵⁵ versus the corresponding atomic mass shows a clear correlation: The heavier are the atoms the lower is their critical limits, see Figure 7. As the atomic weight relates to the size of the atoms and to the number of their outer electrons, such a relationship—which has been suggested long ago as reviewed by Lux¹—can be easily associated with adsorption of these elements at the graphite surface. Even though some mechanisms for their action have been suggested here in and in previous work, they are essentially speculative and would need further analysis to be accepted.

Acknowledgments

Thanks are due to K. Theuwissen, J. Sertucha, J. Bourdie, M. Castro and L. Magnusson Åberg for comments and discussion.

REFERENCES

1. B. Lux, *AFS Cast Metals Res. J.* **8**, 25 (1972)
2. Z. Jiyang, *China Foundry* **7**, 76 (2010)
3. A. Reynaud, *Oligo-éléments et fontes* (ETIF, Sèvres, 2005), pp. 3–147
4. Cast Irons, *ASM Specialty Handbook*, 1st edn. (Materials Park, ASM Int., 1996), pp. 59–60
5. T. Skaland, Nucleation mechanism in ductile iron, in *AFS Cast Iron Inoculation Conference*, pp. 13–30, 2005
6. T. Skaland, O. Grong, T. Grong, *Metal. Trans. A* **24A**, 2321 (1993)

7. T. Skaland, AFS Trans. 01-078 (2001)
8. O.M. Suarez, R.D. Kendrick, C.R. Loper, Int. J. Cast Metals Res. **13**, 135 (2000)
9. Y. Igarashi, S. Okada, Int. J. Cast Metals Res. **11**, 83 (1998)
10. M.J. Lalich, J.R. Hitchings, AFS Trans. **84**, 653 (1976)
11. H. Nakae, Y. Igarashi, Mater. Trans. **43**, 2826 (2002)
12. J.K. Solberg, M.I. Onsoien, Mater. Sci. Tech. **17**, 1238 (2001)
13. J.C. Mercier, R. Paton, J.C. Margerie, C. Mascré, Fonderie **277**, 191 (1969)
14. H. Horie, T. Kowata, A. Chida, Cast Metals **1**, 90 (1988)
15. B. Francis, Metall. Trans. A **10A**, 21 (1979)
16. T. Kusakawa, Adv. Mater. Res. **4–5**, 61 (1997)
17. K. Theuwissen, L. Laffont, M. Véron, J. Lacaze, Int. J. Cast Metals Res. **29**, 11 (2016)
18. M. Hecht, E. Nonon, Int. J. Cast Met. Res. **16**, 307 (2003)
19. R. Suárez, J. Sertucha, P. Larrañaga, J. Lacaze, Metall. Mater. Trans. B **47B**, 2744 (2016)
20. M.I. Onsoien, O. Grong, T. Skaland, K. Jorgensen, Mater. Sci. Tech. **15**, 253 (1999)
21. S.E. Franklin, R.A. Stark, Mat. Res. Soc. Symp. Proc. **34**, 25 (1985)
22. J.S. Park, J.D. Verhoeven, Metall. Mater. Trans. A **27A**, 2740 (1996)
23. K. Theuwissen, J. Lacaze, L. Laffont, J. Zollinger, D. Daloz, Trans. Indian Inst. Met. **65**, 707 (2012)
24. K. Theuwissen, Etude de l'influence des impuretés et des éléments à l'état de traces sur les mécanismes de croissance du graphite dans les fontes. (PhD thesis, INP-Toulouse, France, 2013)
<http://ethesis.inp-toulouse.fr/archive/00002393/>. Accessed 8 Sept 2016
25. K. Theuwissen, J. Lacaze, L. Laffont, Carbon **96**, 1120 (2016)
26. R. Mitsche, G. Haensel, K. Maurer, H. Schäffer, Fonderie **270**, 367 (1968)
27. B. Miao, D.O. Northwood, W. Bian, K. Fang, M.H. Fan, J. Mater. Sci. **29**, 255 (1994)
28. Den Xijun, Zhu Peiyue, Liu Qifu, in *The Physical Metallurgy of Cast Iron*, ed. by H. Fredriksson, M. Hillert (North-Holland, New York, 1985), p. 141
29. G.F. Geier, W. Bauer, B.J. McKay, P. Schumacher, Mater. Sci. Eng. A **413–414**, 339 (2005)
30. J. Lacaze, K. Theuwissen, L. Laffont, M. Véron, IOP Conf. Ser. Mater. Sci. Eng. **117**, 012024 (2016)
31. P.C. Liu, C.L. Li, D.H. Wu, C.R. Loper, AFS Trans. **91**, 119 (1983)
32. K. Theuwissen, M.C. Lafont, L. Laffont, B. Viguier, J. Lacaze, Trans. Indian Inst. Met. **65**, 627 (2012)
33. K. Theuwissen, J. Lacaze, M. Véron, L. Laffont, Mater. Char. **95**, 187 (2014)
34. R. Ghergu, L. Magnusson Åberg, J. Lacaze, Mater. Sci. Forum **790–791**, 435 (2014)
35. G.X. Sun, C.R. Loper, AFS Trans. **91**, 841 (1983)
36. R.A. Sidorenko, V.I. Chermenskiy, M.D. Kharchuk, Russ. Metall. **3**, 42 (1974)
37. J.E. Rehder, American Foundryman **21**, 44 and 57 (1952)
38. H. Fidos, FWP J. **7**, 39 (1977)
39. H. Fidos, FWP J. **22**, 43 (1982)
40. J. Lacaze, N. Valle, K. Theuwissen, J. Sertucha, B. El Adib, L. Laffont, Advances in Materials Science and Engineering, (2013), Article ID 638451. doi: [10.1155/2013/638451](https://doi.org/10.1155/2013/638451)
41. F. Songlin, R. Mingin, Z. Jieqing et al., Nucl. Instrum. Methods Phys. Res. B **104**, 557 (1995)
42. I. Minkoff, *The Physical Metallurgy of Cast Iron*, 1st edn. (Wiley, Chichester, 1983), pp. 159–174
43. A. Munitz, S. Nadiv, J. Mater. Science **17**, 3409 (1982)
44. N. Valle, K. Theuwissen, J. Sertucha, J. Lacaze, IOP Conf. Ser. Mater. Sci. Eng. **27**, 012026 (2011)
45. I. Minkoff, B. Lux, in *The metallurgy of cast iron*, ed. by B. Lux, I. Minkoff, F. Mollard (Georgi Publishing Company, St Saphorin, 1975), p. 473
46. V. Gerval, J. Lacaze, ISIJ Int. **40**, 386 (2000)
47. J. Lacaze, S. Ford, C. Wilson, E. Dubu, Scand. J. Metal. **22**, 300 (1993)
48. A. Freulon, P. de Parseval, C. Josse, J. Bourdie, J. Lacaze, Metall. Mater. Trans. A **47A**, 5362 (2016)
49. J. Lacaze, J. Sertucha, L. Magnusson-Åberg, ISIJ Int. **56**, 1606 (2016)
50. J. Lacaze, Int. J. Cast Met. Res. **11**, 431 (1999)
51. T. Thielemann, Giessereitechnik **16**, 16 (1970)
52. J. Lacaze, J. Sertucha, Int. J. Cast Met. Res. **29**, 74 (2016)
53. D.D. Double, A. Hellawell, Acta Metal. Mater. **43**, 2435 (1995)
54. P. Dierickx, C. Verdu, A. Reynaud, R. Fougères, Scr. Mater. **34**, 261 (1996)
55. L. Magnusson Åberg, C. Hartung, J. Lacaze, Trace elements and the control limits in ductile iron, in *Proceedings of the 10th International Symposium Science and Processing of Cast Irons*, <http://rinfi.fi.mdp.edu.ar/xmlui/handle/123456789/28>. Accessed 1 June 2015
56. R.D. Maier, J.F. Wallace, AFS Trans. **84**, 687 (1976)
57. B. Lux, W. Kurz, ISI Publ. **110**, 193 (1969)
58. F. Lietaert, Giessereiforschung **49**, 106 (1997)
59. H. Nakae, Ying Zou, Y. Sato, Influence of graphite morphology, thermal history and S and Cu on ferrite/pearlite formation in cast iron, in *Proceedings of the 72nd World Foundry Congress*, 1996, paper SL-2
60. Y. Zou, Influence of alloying elements and melting conditions on graphite morphology and matrix in Fe–C and Ni–C alloys. (PhD Thesis, Waseda university, 2012)
<https://dspace.wul.waseda.ac.jp/dspace/bitstream/2065/40286/1/Honbun-6022.pdf>. Accessed 8 Sept 2016
61. A. Schneider, H. Viehhaus, G. Inden, H.J. Grabke, E.M. Müller-Lorenz, Mater. Corros. **49**, 336 (1998)
62. D.J. Young, J. Zhang, C. Geers, M. Schütze, Mater. Corros. **62**, 7 (2011)

63. J.L. Zubimendi, R.C. Salvarezza, L. Vasquez, A.J. Arvia, *Langmuir* **12**, 2 (1996)
64. J.L. Vicente, E.E. Mola, G. Appignanessi, J.L. Zubimendi, L. Vasquez, R.C. Salvarezza, A.J. Arvia, *Langmuir* **12**, 19 (1996)
65. A. Agüero, M. Guitierrez, L. Korcakova, T.T.M. Nguyen, B. Hinnemann, S. Saadi, *Oxid. Met.* **76**, 23 (2011)
66. I. Baumer, *Private discussion* (Tupy Foundry, Joinville, Brazil, 2014)
67. M. Gorny, in *Encyclopedia of Iron, Steel, and Their Alloys*, ed. By R. Colás, G.E. Totten (CRC Press, 2016) p. 718